

## Article

# Carbon Accumulation and the Possibility of Carbon Losses by Vertical Movement of Dissolved Organic Carbon in Western Siberian Peatlands

Evgeny A. Zarov <sup>1</sup>, Elena D. Lapshina <sup>1</sup>, Iris Kuhlmann <sup>2</sup> and Ernst-Detlef Schulze <sup>2,\*</sup>

<sup>1</sup> Laboratory of Ecosystem-Atmosphere Interactions of the Mire-Forest Landscapes, Yugra State University, 628007 Khanty-Mansiysk, Russia; zarov.evgen@yandex.ru (E.A.Z.); e\_lapshina@ugrasu.ru (E.D.L.)

<sup>2</sup> Max Planck Institute for Biogeochemistry, 07743 Jena, Germany; kuhlmann@bgc-jena.mpg.de

\* Correspondence: dschulze@bgc-jena.mpg.de

**Abstract:** We studied the peat stratigraphy of the Mukhrino peatland, which is a typical ombrotrophic bog for the Middle Taiga zone of Western Siberia, to gain insights into its history, hydrology, and carbon fluxes. For the first time in Western Siberia, seven cores were collected from locations that were chosen to represent the typical present-day vegetation types, and this was performed for the dating of the separated dissolved (DOC) and particulate organic carbon (POC) fractions, which were determined using the Accelerator Mass Spectrometer (AMS) radiocarbon (<sup>14</sup>C) method. The oldest peat was found at the bottoms of an underlying lake (10,053 cal. year BP) and an ancient riverbed (10,989 cal. year BP). For the whole history of the peatland, the average peat accumulation rate was estimated to be  $0.067 \pm 0.018$  cm yr<sup>-1</sup> (ranging from 0.013 to 0.332 cm yr<sup>-1</sup>), and the carbon accumulation rate was  $38.56 \pm 12.21$  g m<sup>-2</sup> yr<sup>-1</sup> (ranging from 28.46 to 57.91 g m<sup>-2</sup> yr<sup>-1</sup>). There were clear age differences between the separated samples of the DOC and POC. The DOC was older than the POC in the uppermost 150 cm of the peat deposit and younger in the deeper layers. The difference in age increased with depth, reaching 2000–3000 years at the bottom of the peat deposit (depth of 430–530 cm). Following the consideration of a range of factors that could potentially cause the dating discrepancy, we hypothesised that the DOC continuously moves down into the mineral sediment beneath the peat, as an additional carbon flux that results in the mixing of younger and older carbon. On this basis, we estimated the apparent rate of the DOC's downward movement and the associated rate of carbon loss. The first estimate of the average rate of the DOC's downward movement in Western Siberia was  $0.047 \pm 0.019$  cm yr<sup>-1</sup>, causing carbon loss in the range of 28–404 mg m<sup>-2</sup> yr<sup>-1</sup>.

**Keywords:** AMS radiocarbon dating; Mukhrino bog; peat accumulation rate; peatland stratigraphy; POC



**Citation:** Zarov, E.A.; Lapshina, E.D.; Kuhlmann, I.; Schulze, E.-D. Carbon Accumulation and the Possibility of Carbon Losses by Vertical Movement of Dissolved Organic Carbon in Western Siberian Peatlands. *Forests* **2023**, *14*, 2393. <https://doi.org/10.3390/f14122393>

Academic Editor: Randall K. Kolka

Received: 12 October 2023

Revised: 22 November 2023

Accepted: 27 November 2023

Published: 7 December 2023



**Copyright:** © 2023 by the authors. Licensee MDPI, Basel, Switzerland. This article is an open access article distributed under the terms and conditions of the Creative Commons Attribution (CC BY) license (<https://creativecommons.org/licenses/by/4.0/>).

## 1. Introduction

Unlike most other ecosystems, peatlands assimilate carbon and sequester it over thousands of years, as long as the net primary production exceeds the rate of organic matter decomposition [1]. It has been estimated that peatlands occupy 2.84% (4.23 million km<sup>2</sup>) of the global land area [2], but they have accumulated a disproportionately considerable amount of the world's soil carbon (~30%) [3].

One of the most-waterlogged territories worldwide is Western Siberia, where peatlands cover ~22% [4] of the total area, and the waterlogging of some lands reaches 50%–75% locally [5]. There, peatlands occupy depressions in local reliefs, vast watershed areas, and floodplains [6]. It is estimated that Western Siberian peatlands contain ~20% of the total world peat deposits, with the highest concentration in the Taiga zone (55° N to 65° N) [4,7]. Moreover, they hold a carbon stock of approximately 70.2 Pg, representing up to ~26% of the total terrestrial organic carbon (which is held in soils, detritus, and vegetation) accumulated since the Last Glacial Maximum [8,9].

Western Siberian peatlands developed mainly during the early Holocene (11,500–9000 cal yr BP) due to postglacial warming [7,8]. The rates of carbon accumulation ranged from  $12 \text{ g m}^{-2} \text{ yr}^{-1}$  to  $39 \text{ g m}^{-2} \text{ yr}^{-1}$  throughout the Holocene, depending on latitude. The average accumulation rate for the Middle Taiga zone is  $28.5 \text{ g m}^{-2} \text{ yr}^{-1}$ , and this generally declines towards older dates [6,10,11]. Exceptions are found in the uppermost 50 cm due to poorly decomposed and uncompressed peat.

The amount of biomass input determines the rate of peat and, consequently, the carbon transfer from the acrotelm (surface aerobic layer) to the catotelm (deep anoxic layer) [12]. This is strongly correlated with climatic conditions [13], as well as with the plant species that form the peat [14]. Thus, the peat accumulation process is not constant in time, and it is determined by organic matter input and its decay rates [12]. During decomposition under waterlogged conditions, parts of the litter and peat convert to a dissolved form, which can pass through a  $0.45 \mu\text{m}$  filter, which is known as dissolved organic carbon (DOC) [15–21], but  $0.2\text{--}0.7 \mu\text{m}$  filter pore sizes are also common [22]. Expected global warming may increase the DOC concentrations in the water discharged to streams [23]; thus, this will ultimately increase the DOC flux into the oceans [24,25], where a significant fraction is rapidly mineralised and returned to the atmosphere as a greenhouse gas. The paths and magnitudes of the DOC fluxes are not accounted for in most estimates of the contributions to the C cycle; thus, they require further scientific attention to support the forecasting of climate change effects.

Most of the DOC released to streams and rivers [25,26] is derived from recently fixed carbon ( $\sim 50$  years) in the upper peatland layers [27]. However, radiocarbon dating has shown that riverine DOC is much older than previously thought [28], thereby suggesting that the baseflow from deeper peats may also export the DOC to streams. This DOC does not flow directly to the mineral floor beneath the peatland, but it moves vertically up and down in the peat profile, and there is a significant redistribution of the DOC in groundwater [29]. Also, any vertical DOC inflow from the upper peatland layers may be converted to  $\text{CO}_2$  and  $\text{CH}_4$  by microbial activity [15,17,18,30,31]. Thus, the waterborne flux of DOC is important in the determination of the peatland carbon budget and in understanding the spatial and temporal variability of  $\text{CO}_2$  and  $\text{CH}_4$ . Vertical movements of the DOC can also lead to the mixing of young and old carbon, which may result in dating inversions and inaccuracies in the bulk samples of peat. Inversed dates are usually excluded from the age–depth model, which may lead to a significant shift in the model shape, which could affect the interpretation [32,33]. Well-known reasons for dating inversions include root intrusion [34], the slippage of neighbouring peat [35], peat fires [36], as well as other profile disturbances [32] such as dry years, cryoturbation, and periodic flooding [37]. Each of these occurs intermittently; however, a permanent downward flux of the DOC is implied by the dating discrepancies reported. This could cause a systematic under-estimation of bulk sample dates, and this may have affected previous estimates of the carbon accumulation rates in peatlands. These considerations create a need for the separate age determinations of the DOC and the immobile particulate organic matter (POM).

Despite the high scientific interest to the carbon cycle topic, a limited amount of information has been found about the DOC dating in the vertical peatland profile, and there was almost a complete lack of data about the vertical DOC distribution through the peatlands. Thus, for the first time in the Western Siberian region, a massive amount of data on the dating of the DOC and POC were collected. The objectives of the study described here were: (1) to describe the stratigraphy, as well as measure the historical peat and carbon accumulation rates at the Mukhrino bog in Western Siberia; (2) to date the dissolved (DOC) and particulate organic carbon (POC) separately throughout the peat profile; (3) if differences in the ages of the DOC and POC at the same depths are found, to explore potential causes and implications.

## 2. Materials and Methods

### 2.1. Study Site

The Mukhrino peatland is located 20 km southwest of Khanty-Mansiysk city in the Middle Taiga zone [38] of Western Siberia near the confluence of two major rivers, the Irtysh and the Ob' (60.889° N, 68.702° E). It covers a local watershed between two smaller rivers—the “Mukhrina” and the “Bolshaya rechka” (Figure 1), within a zone of ombrotrophic (rainfed) *Sphagnum* raised bogs on the left terrace of the River Irtysh [39]. Covering an area of 65 km<sup>2</sup>, the Mukhrino peatland hosts a field station that is operated by the UNESCO Chair of Environmental Dynamics and Global Climate Change at Yugra State University.

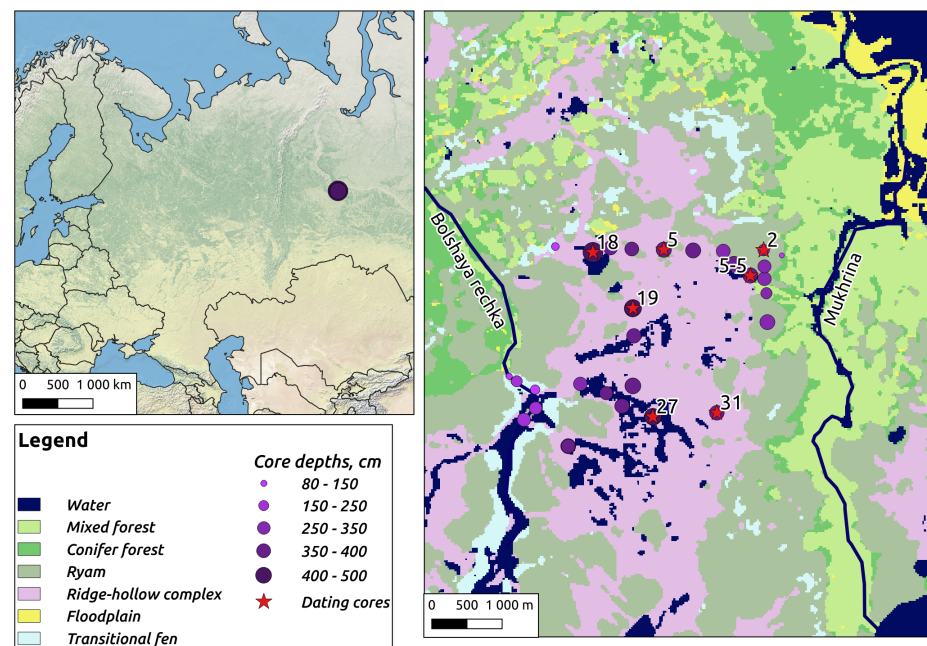


**Figure 1.** Maps showing the location of the Mukhrino peatland on the map of Eurasia (left) and the distribution of peat cores in relation to the main ecosystems of the study area and bounding rivers (right). Several cores, both collected at the adjacent hollow and ridge, are presented as a single dot on the map.

The climate of the region is moderately continental. According to Russian Weather Service observations at the Khanty-Mansiysk weather station, the mean annual air temperature is  $-1.0$  °C. Winter is cold, with the mean January temperature being  $-21.5$  °C; summer is short with the mean July temperature reaching  $17.4$  °C [40]. The mean annual precipitation is 480 mm, and most (307 mm) of this amount falls during the summer–autumn season (August–September). The remaining precipitation falls as snow, starting in October. The snow begins to melt in mid-April and disappears completely in May. The area is characterised by the absence of permafrost; however, in some places, frozen soil can be found at depths of 50–100 cm until the end of June.

The peatland is surrounded by Taiga forest dominated by *Pinus sibirica*, *Picea obovata*, and *Abies sibirica* mixed with *Populus tremula* and *Betula pubescens*, which occupies the mineral islands and slopes along the rivers and streams. The following contemporary peatland vegetation types are present:

- **Typical ryam** (pine–dwarf shrub–peat moss community) is characterised by a low Scots pine layer (*Pinus sylvestris* f. *litwinivii*, height 1.5–4 m), a well-developed dwarf shrub layer (*Ledum palustre*, *Chamaedaphne calyculata*), and a moss layer dominated by *Sphagnum fuscum* with a minor admixture of *S. angustifolium* and *S. divinum*;

- **Tall ryam**, which is found on shallower peat near the outer edges of the peatland, is similar to the typical ryam, except that it has tall pine trees (*Pinus sylvestris f. uliginosa*, height 6–10 m) and *Sphagnum angustifolium* dominates the moss layer;
- **The ridge–hollow complex** features ridges, which are elongated perpendicular to the water flowlines; they are occupied by typical ryam communities, alternating with waterlogged sedge–peat moss hollows (*Carex limosa*, *Scheuchzeria palustris*, *Eriophorum russeolum*, *Sphagnum balticum*, *S. majus*, *S. jensenii*);
- **Treeless throughflow fens**, as well as *Sphagnum* lawns with hollow vegetation and occasional scattered hummocks, which are located within limited areas in the lower reaches of the peatland water catchment [41].

The peatland has a domed shape with an elevation difference of 1.2 m between the central part and the edge [16]. The central part of the dome is relatively flat; it is occupied by the ridge–hollow complex, whereas towards the edge, it becomes more inclined and better drained with ryam and tall ryam communities.

The Mukhrino peatland receives water from rainfall and melting snow. Usually, meltwater is retained on the peatland surface in local depressions or upstream of ridges until the upper peat layer has thawed. When surface ice breaks up, the meltwater rapidly seeps into the peat, which raises the water table dramatically. The lowest water level is recorded at the end of summer (in August). The water table rises again in response to precipitation during the autumn season, which is characterised by low air temperature and reduced evapotranspiration. Discharge from the peatland stops in the middle of October when water freezes. For more information, see Bleuten [6].

## 2.2. Field Sampling

To describe the peatland stratigraphy, 34 peat cores were collected in 2010–2016 using a Russian peat corer (chamber length of 0.5 m, inside diameter of 5.0 cm). Each core was extracted from a single borehole, and sampling continued through the entire depth of the peat until the bottom sediment was reached. The locations of the cores were chosen to include the most-typical and the most-unique habitats of the Mukhrino peatland (Figure 1). The uppermost 50 cm layer was extracted in the same way, but with some gaps due to the fragile structure of the litter and living mosses. The gaps were mostly related to the first 20–30 cm layer. If a gap occurred in the lower sections of the core, the peat sample was manually extracted using a knife, and no dating was performed on these sections.

In the summer of 2016, seven additional peat cores were extracted from the most-typical bog habitats (Table 1) using the same methodology. From near the lower end of each half-metre section of each core, we cut a 1 cm-thick slice (in total, 67 samples; see the Supplementary Materials for exact depths, Table S1). Using a clean knife, we transferred these pieces into labelled plastic zip-bags, taking care to minimise contact with the environment and to prevent contamination. The remainder of each core section was placed in a plastic cassette and wrapped in plastic film. All samples were then transported to the laboratory of Yugra State University (Khanty-Mansiysk, Russian Federation). The zip-bags with the contents were immediately frozen, then sent in insulated packaging to the Max-Planck Institute of Biogeochemistry in Jena (Germany), where they were kept frozen until analysis (separation of the DOC and POC followed by AMS radiocarbon dating) in January 2018. The fresh material from the cassettes was divided into 10 cm subsamples to conduct analyses in Khanty-Mansiysk.

**Table 1.** Habitat descriptions for the seven dating cores (for their locations, see Figure 1). WT = water table.

Core	Habitat Description	WT Depth (cm)	Peat Depth (cm)
2	Typical transition from ryam to dry peatland; covered by pine trees up to 3 m tall, dwarf shrubs ( <i>Ericaceae</i> ), and <i>Sphagnum fuscum</i> .	20–30	530
5, 19	Ridge in ridge–hollow complex; covered by low pine (up to 2 m tall), dwarf shrubs ( <i>Ericaceae</i> ), and <i>Sphagnum fuscum</i> .	15–20	390, 400
5-5	Ecotone between ridge and hollow; covered by mixed species from both habitats: cottongrass, <i>Sphagnum</i> mosses ( <i>S. fuscum</i> , <i>S. balticum</i> ), dwarf shrubs ( <i>Ericaceae</i> ).	5–10	310
18	Floating <i>Sphagnum</i> mat close to the lake; covered by <i>Scheuchzeria</i> , sedges ( <i>Carex limosa</i> ), and <i>Sphagnum</i> mosses ( <i>S. papillosum</i> , <i>S. balticum</i> ).	2–5	480
27	Ridge in ridge–pool complex; treeless ridge with dwarf shrubs and <i>Sphagnum</i> mosses.	10–15	400
31	Hollow in ridge–hollow complex; covered by sedges ( <i>Carex limosa</i> ) and <i>Sphagnum balticum</i> .	5–10	380

### 2.3. Identification of Peat Types

Plant macrofossils were analysed in contiguous 10 cm subsections of all cores. For this purpose, a subsample of 10 cm<sup>3</sup> (10 cm height, 1 cm width, 1 cm thickness) was washed with flowing water through a 0.25 mm mesh sieve. We identified plant remains under a binocular microscope (10–40× magnification; Zeiss Axiostar, Jena, Germany) following a protocol [42,43] and using the key samples data bank, i.e., the collection of plant remains that were found in the region and used for peat botanical composition identification (unpublished). The abundance of each type of plant remains was expressed as a percentage, and peat types were identified based on the dominance of plant species according to Matukhin [44].

### 2.4. Bulk Density, Carbon, and Ash Content

The bulk density, carbon, and ash content of each 10 cm subsample were determined on 50 cm<sup>3</sup> of peat that was taken from the middle 5 cm (2.5–7.5 cm) of the core section. Bulk density (BD; g cm<sup>−3</sup>) was measured by drying this peat at 105 °C for 24 h, weighing, and dividing by the initial volume. The dried subsample was ground and divided into two parts. Ash content was determined (for one part) by ignition (Nabertherm L9/11/SKM, Lilienthal, Germany) at 525 °C for 9 h. The second part was used to determine the total carbon content (elemental analyser EA-3000; EuroVector, Pavia, Italy). When the samples were introduced to this analyser and combusted, the carrier gas helium was temporarily mixed with pure oxygen. The gases were separated by a system similar to that of gas chromatography (purge and trap principle). Being released from the adsorption column,

carbon dioxide was measured by the thermal conductivity detector (TCD). The instrument was calibrated with Atropine (C = 70.56%, N = 4.84%, H = 8.01%, O = 16.59%). Concerning the seven dating cores that were collected in 2016, the bulk density and ash content were measured only on Cores 5, 5-5, 19, and 27, while the carbon content was measured on Cores 2, 5, 5-5, and 19 (Figure 1), which was sufficient to cover all peat types.

### 2.5. Separation of DOC and POC

At the laboratory in Germany, the DOC was separated from the POC by dispersing the peat samples in distilled water using the approach from Schulze et al. (2015). Dissolved organic carbon (DOC) is operationally defined as organic molecules that can pass through a 0.45 µm filter [22]. In our separation setup for the peat samples, the smallest available glass fibre filter of 1.6 µm was chosen, which is specifically required for <sup>14</sup>C analysis. Therefore, in our setup, the DOC was considered as organic particles that can pass through a 1.6 µm glass fibre filter. First, the frozen peat sample was thawed carefully, weighed, dispersed in distilled water, and shaken for two hours. The suspension was then wet-sieved (63 and 36 µm mesh), and the residues were freeze-dried (Piatkowski, Munich, Germany). The sieved suspension (<36 µm) was adjusted to pH 9 by adding NaOH, shaken for another 20 min, and centrifuged at 2900 × g for 30 min (Megafuge 3.0, Heraeus, Hanau, Germany). The supernatant was vacuum-filtered through a 1.6 µm glass fibre filter (Sartorius), which had been baked at 500 °C beforehand, and the filtrate (<1.6 µm) was freeze-dried. The residue from the filter and the pellet remaining from the centrifugation were combined and freeze-dried. This fraction, which had a particle size between 1.6 and 36 µm, is defined as the particulate organic carbon (POC).

### 2.6. AMS <sup>14</sup>C Analysis

The DOC and POC samples from the peat cores were analysed using the Accelerator Mass Spectrometer (AMS) radiocarbon (<sup>14</sup>C) method [45,46]. For one measurement, 0.7 mg of carbon (C) was required. The samples were chemically prepared by combustion to produce CO<sub>2</sub>, which was trapped and catalytically reduced to graphite in the presence of Fe<sup>2+</sup> powder and H<sub>2</sub>. The resulting graphite was pressed into the targets for measurement in the AMS system, and therein, it was ionised (negative charge) and accelerated within an electric field to a final energy of 400 keV. The <sup>14</sup>C isotope ratios were corrected using the measured 13/12C AMS values [46]. The radiocarbon dates were calibrated (see the Supplementary Materials, Table S1) with the IntCal20 [47] and NH1 post-bomb [48] atmospheric curves using the package ‘clam’ [49]. The age–depth model was developed using the Bayesian-based package ‘rbacon’ [50] with 95 % confidence intervals.

### 2.7. Calculation of Accumulation Rates

The peat accumulation rate (PA) was calculated along the entire core, for each of the dating steps (usually at intervals of approximately 50 cm, but more widely spaced in cases of missing age data; see the Supplementary Materials) using Equation (1):

$$PA_i = \frac{(d_l - d_u)}{(a_l - a_u)}, \quad (1)$$

where PA<sub>*i*</sub> (cm yr<sup>−1</sup>) is the peat accumulation rate for the *i*th time interval between dated samples, while *d<sub>l</sub>*, *d<sub>u</sub>* (cm) are the depths and *a<sub>l</sub>*, *a<sub>u</sub>* (years) are the ages (dates) of the lower and upper surfaces of the corresponding peat layer, respectively.

The short-term apparent carbon accumulation rate (ACAR) was calculated for each 10 cm-depth interval (slice) of the cored profile by Equation (2):

$$ACAR_j = (BD_j \times LOI_j \times CC_j) \times PA_i \times 10^4, \quad (2)$$

where ACAR<sub>*j*</sub> (g m<sup>−2</sup> yr<sup>−1</sup>) is the short-term carbon accumulation rate for the *j*th 10 cm slice, BD<sub>*j*</sub> (g m<sup>−3</sup>) is the bulk density of peat in the *j*th 10 cm slice, LOI<sub>*j*</sub> is the loss on

ignition expressed as a proportion (e.g., 0.9),  $CC_j$  is the proportion of carbon in the organic part of the peat,  $PA_i$  (from Equation (1)) is assumed to apply to all 10 cm core slices that accumulated during the the  $i$ th time interval, and  $10^4$  is a conversion factor (the number of  $\text{cm}^2$  in a  $1 \text{ m}^2$ ). The equation was adapted from [51] by adding the LOI as a correction factor to convert the ACAR results to ash-free organic matter values. In the case of low ash content (i.e., LOI close to unity), this correction had almost no effect; however, in the case of high ash content (i.e., the LOI was 0.5–0.7), it reduced the ACAR to reflect the fact that carbon was accumulated in the organic matter, but not in the mineral fraction. The bulk density, ash content, and carbon content were not all measured in Cores 2, 18, 27, and 31 (see above), so for these cores, the ACAR was calculated at least partly on the basis of peat types, using the mean values of the bulk density, carbon, and ash contents for each peat type, which was derived from a statistical analysis of the 34 cores from the Mukhrino peatland (see the Supplementary Materials, Table S2). However, more-advanced methods of soil carbon stock dynamics analysis using machine learning were presented in [52].

The long-term (apparent) rate of carbon accumulation (LORCA) was calculated according to Borren [12,53] by Equation (3):

$$LORCA = \frac{C_{total}}{A_{bottom}}, \quad (3)$$

where LORCA is the long-term rate of carbon accumulation ( $\text{g m}^{-2} \text{ yr}^{-1}$ ) and  $A_{bottom}$  is the bottom age of the core (years).  $C_{total}$  is the total carbon storage per unit area ( $\text{g m}^{-2}$ ), and it was calculated via the cumulative sum of carbon storage in contiguous 10 cm slices of the peat profile, working from bottom to top (see the Supplementary Materials, Table S2).

The long-term peat accumulation rate (IPA) was calculated using Equation (4):

$$IPA = \frac{D_{total}}{A_{bottom}}, \quad (4)$$

where IPA is the long-term peat accumulation rate ( $\text{cm yr}^{-1}$ ) and  $D_{total}$  is the total depth of the core (cm).

## 2.8. Calculation of DOC Downward Velocity

We hypothesised that, if a dating discrepancy between the DOC and POC at the same depth was found, it could be caused by the DOC's vertical movement within the peat profile. Specifically, if it emerged that the DOC was systematically younger than the POC, this might reflect a continuous downward movement of the DOC relative to the peat matrix. Assuming that the POC is stationary and associated with the solid phase (peat), whereas the DOC is mobile and associated with the liquid phase (peatland water), the apparent rate of the DOC's downward movement could then be calculated according to Equation (5):

$$v = \frac{(d_i - d_{doc_i})}{(a_{poc} - a_{doc})}, \quad (5)$$

where  $v$  is the apparent rate of DOC movement ( $\text{cm yr}^{-1}$ ),  $d_i$  (cm) is the  $i$ th depth from which the DOC was extracted,  $d_{doc_i}$  (cm) is the depth at which the POC was of the same age as the DOC at  $d_i$ , while  $a_{poc}$  and  $a_{doc}$  (years) are the respective ages of the POC and DOC at  $d_i$ . Equation (5) calculates how fast the DOC moved downward during the time period under consideration, regardless of the physical processes that were involved—whether sorption/desorption, dissolution/sedimentation, microorganism consumption, or changes in substrate porosity. Then, the amount of carbon that was lost as a result of the DOC downward movement is given by Equation (6):

$$cc = C \times v \times 10^4, \quad (6)$$

where  $cc$  ( $\text{mg m}^{-2} \text{yr}^{-1}$ ) is the amount of carbon lost per square metre and  $C$  ( $\text{mg cm}^{-3}$ ) is the DOC concentration in the deep peatland water. This concentration ranged between  $0.06 \text{ mg cm}^{-3}$  [54] and  $0.2 \text{ mg cm}^{-3}$  [55], and  $10^4$  is a conversion factor, as above.

### 3. Results

#### 3.1. Stratigraphy

After the last glaciation, the Mukhrino peatland started as a minerotrophic fen dominated by trees (birch, pine, fir) and herbs (fern, horsetail, and tussock-forming sedges). Remains of these plants are found in the bottom layer of the minerotrophic peat. The thickness of this layer does not exceed 1.7 m, being 0.65 m on average. It is overlain by  $\sim 0.5$  m of transitional peat, which contains minerotrophic plant remains (*Scheuchzeria palustris*, sedges, dwarf shrubs, and *Sphagnum* mosses). Ombrotrophic peat forms the main upper part of the peatland (Figure 2). About two-thirds of the peat deposit is composed of *Sphagnum* peat. The thin interlayers of cottongrass–*Sphagnum* or sedge–*Scheuchzeria*–*Sphagnum* peat types, are formed by dynamic changes in the ridge–hollow complex. The most-abundant types are *Sphagnum fuscum* peat (22.5 % of the entire peat deposit), *Sphagnum* hollow peat (*S. balticum*, *S. papillosum*; 12.0 %), and mixed *Sphagnum* ombrotrophic peat (*S. fuscum*, *S. angustifolium*, *S. divinum*, *S. papillosum*, *S. balticum*; 5.7 %).

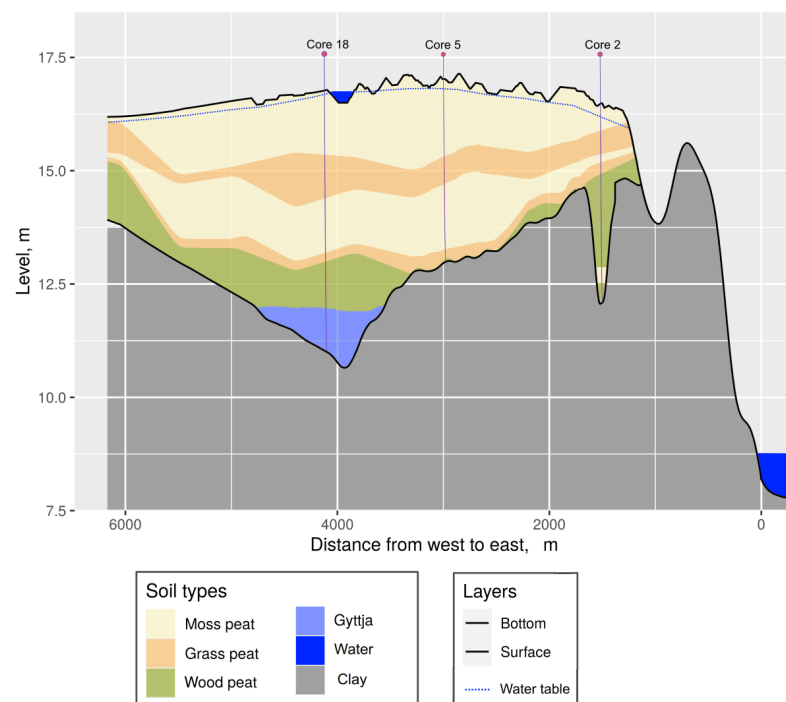


**Figure 2.** Section through the Mukhrino peatland showing the stratigraphy and shape of the mineral bottom.

#### 3.2. Peat Ages and Accumulation Rates

The average depth of the Mukhrino peatland is 340 cm, with 34 cores ranging in length from 85 to 530 cm (Figures 1–3; see the Supplementary Materials, Table S2). The two deepest points were found in the northern part of the peatland: Core 18 is located in the basin of a primary lake (peat depth of 480 cm), which is partly infilled by gyttja (100 cm) covered with peat (380 cm); Core 2 (peat depth of 530 cm) is associated with an ancient stream bed with rush peat at the bottom. Other cores have 40–60 cm of minerotrophic grass–woody peat at the bottom (depths of 350–400 cm).

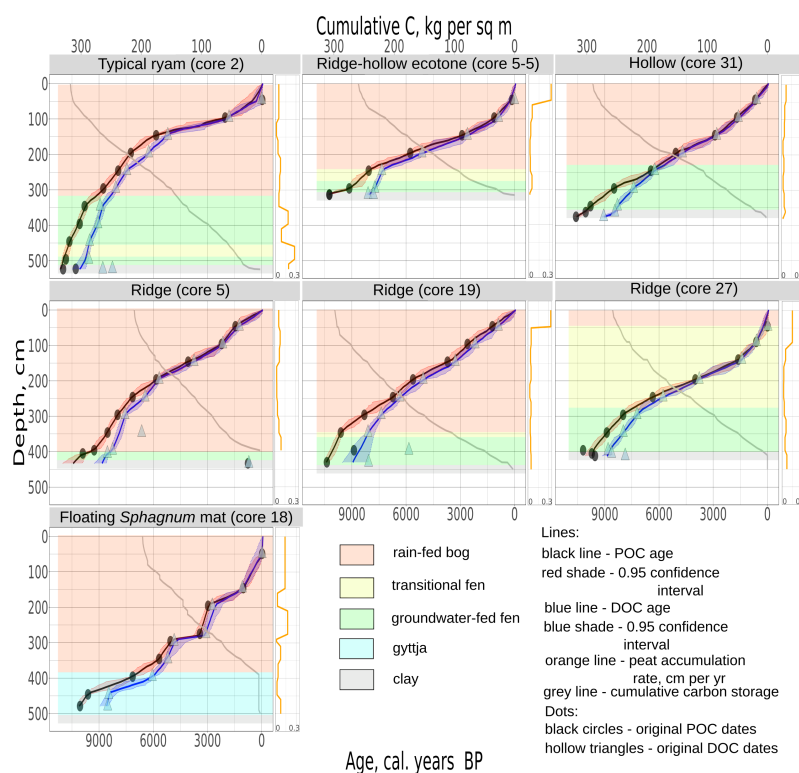


**Figure 3.** The age–depth models, carbon accumulation curves, and peat types for the seven dating cores from the Mukhrino peatland.

Shallow peat deposits ( $\sim 100$  cm and less) are present at the edges of the peatland that is bordered by forest and mineral islands. The peatland is still expanding by paludification of the surrounding forest area, where an abundance of tall, dry, and dead conifer trunks is found on shallow peat deposits. The abundance of charcoal in the peat may be attributed to frequent fire events at the bog edge, and the presence of *Carex globularis* in the modern vegetation is also an indicator of fires [33]. Usually, this fire type does not reach the central part of the peatland and destroys only treed areas at the border with forest growing on mineral soils.

The average PA is  $0.067 \pm 0.02$  cm yr<sup>-1</sup> (the data used for this calculation can be found in the Supplementary Materials). The lowest average value ( $0.04 \pm 0.02$  cm yr<sup>-1</sup>) was found for Core 31 (hollow), and the highest average value ( $0.10 \pm 0.08$  cm yr<sup>-1</sup>) was found for Core 2 (ryam). The PA was the highest for ombrotrophic peat ( $0.080 \pm 0.038$  cm yr<sup>-1</sup>), lower in minerotrophic peat ( $0.062 \pm 0.033$  cm yr<sup>-1</sup>), and the lowest for transitional peat ( $0.061 \pm 0.027$  cm yr<sup>-1</sup>). Apparently, the type of water (rainwater or groundwater) and nutrient availability are amongst the main limiting factors in the peat-accumulation process.

The range of average the IPA values was 0.03–0.048 cm yr<sup>-1</sup> (the mean value  $0.041 \pm 0.007$  cm yr<sup>-1</sup>), depending on the total depth; i.e., peat accumulation over 10–11 kyr was 1.2–1.6-times faster for the deepest cores than for the shallow cores. The average PA based on 64 dates over different peat layers across all cores had a higher value of  $0.067 \pm 0.018$  cm yr<sup>-1</sup> ( $0.013$ – $0.332$  cm yr<sup>-1</sup>), mostly owing to increased rates ( $0.137$ – $0.332$  cm yr<sup>-1</sup>) of recent (from 600 BP to present day) peat accumulation for several cores.

High rates of peat accumulation were found in the bottom minerotrophic layers of Core 2 ( $0.086$ – $0.277$  cm yr<sup>-1</sup>). The PA value started to decrease to  $0.049$  cm yr<sup>-1</sup> at approximately 9800 cal years BP when the vegetation changed from minerotrophic to a transition type. The highest PA values during the last  $\sim 1200$  years were calculated for Core 5-5 ( $0.332$  cm yr<sup>-1</sup>) and Core 19 ( $0.336$  cm yr<sup>-1</sup>), which were located on *Sphagnum fuscum* ridges (water table depth of 30–40 cm) in the ridge–hollow complex. During the same

period, increased PA values were calculated for Cores 18 and 27 (0.137 and 0.147 cm yr<sup>-1</sup>, respectively), where water levels were apparently higher because *Sphagnum papillosum* dominated the moss layer. In general, the PA values decreased between 6500 and 3000 cal yr BP and increased for older and younger dates, reaching maximum values in current times (Figures 3 and 4).

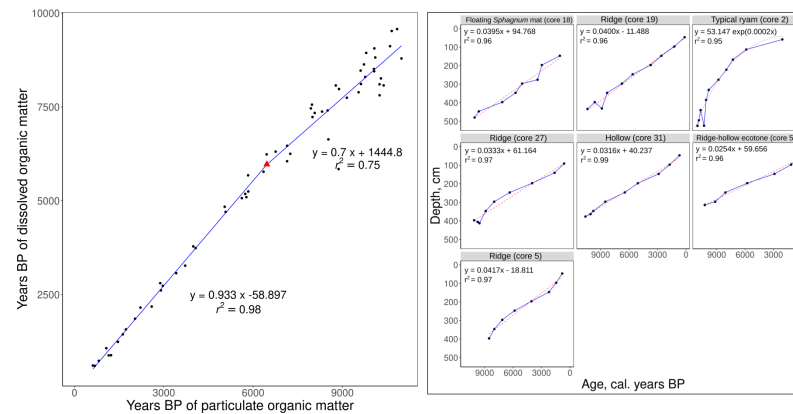


**Figure 4.** A scatter plot of the correlation coefficient between the DOC and POC ages (left). The red triangle is a breaking point of linear regression. The age–depth models of the POC with the regression equations and  $r^2$  (right).

The oldest peat layers were found in Cores 2 and 18 (~11,000 and 10,000 cal yr BP), which means the peat accumulation process started from the eastern and western edges of the area now occupied by peatland and encroached onto its central part during the next 1500–2500 years. Thus, the lateral rate of peatland expansion can be estimated at 0.65–1.0 m yr<sup>-1</sup> during the period 11,700–8200 cal yr BP.

The oldest peat was formed 10,989 cal yr BP, and the oldest gyttja was deposited 10,053 cal yr BP. In general, peat growth started via terrestrialisation after lake sediments had filled the lake basin, between 7000 and 6000 cal yr BP. Based on eight dates from the deepest peat layers, the average date of the peatland initiation was 10,265 cal yr BP (see Supplementary Materials, Table S1).

### 3.3. Bulk Density and Ash Content

BD values increased linearly with depth from 0.016 to 0.348 g cm<sup>-3</sup> (see the Supplementary Materials, Table S2), which was caused mainly by changes in the peat stratigraphy. Ombrotrophic *Sphagnum* moss peat types have the lowest BD values because they have a low decomposition rate and, thus, retain more of their initial volume [56]. In the Mukhrino peatland, many well-preserved *Sphagnum fuscum* peats (decomposition degree 5%–10%, H1–H2 von Post) were found at depths greater than 200 cm, overlain by more-decomposed layers. On the other hand, minerotrophic peat contains much woody and sedge remains, which, over time, lose structure to create dense peat layers and may mix with mineral sediments at the bottom [57].

Ash content changed irregularly with a maximum (5%–8%) at a 100 cm depth followed by a subsequent decline (~2.5%), then slowly increased again towards the mineral bottom (5%–7%). These variations are related to the composition of the plant remains. The ombrotrophic *Sphagnum* peat types have the lowest ash content, while herb and wood peats normally show high ash content values [57].

In all of the Mukhrino peat cores, we measured high ash content in the upper peatland layers (50–100 cm) [10,33]. This might be explained by mineral sediments covering the peatland during an extreme flooding event 1000–2000 years ago or by a surface fire. However, the analysis of the soil and peat composition to elucidate the fire history of the Mukhrino peatland gave no indication of a large fire event during the last 1300 years [33]. No historical

evidence about extreme flooding in the region was found. Therefore, additional exploration is needed.

### 3.4. Carbon Accumulation Rate

The range of LORCA values was 24.80–28.92 g m<sup>-2</sup> yr<sup>-1</sup> (average 26.93 ± 1.76 g m<sup>-2</sup> yr<sup>-1</sup>). The ACAR is determined by a high PA (0.15–0.33 cm yr<sup>-1</sup>) in the upper peat layers and by a high BD (0.4–1.4 g cm<sup>-3</sup>) in the lower layers. The average ACAR for all seven cores was 37.99 ± 11.4 g m<sup>-2</sup> yr<sup>-1</sup>, and the median value was 26.17 g m<sup>-2</sup> yr<sup>-1</sup>. These values are similar to the average values for the middle boreal zone of Western Siberia (24.8 ± 5.5 g m<sup>-2</sup> yr<sup>-1</sup>) [58]. The average C content for the 10 cm peat slice was 6.16 ± 1.46 kg m<sup>-2</sup>. The total amount of C stored up to the average depth (4.3 m) was 264.9 ± 62.8 kg m<sup>-2</sup>.

### 3.5. POC and DOC

The DOC and POC dates were closely correlated (Pearson linear correlation,  $r^2 = 0.98$ , slope 0.93) from the present time until ~6000 cal year BP, when they started to diverge (Figure 4). In older peat layers, the slope of the relationship between the DOC and POC ages (Figure 4) decreased (to 0.7), with increasing variation ( $r^2 = 0.75$ ). Differences between the DOC and POC ages showed a linear relationship with depth (Pearson linear correlation,  $r^2 = 0.55$ , slope 0.14) and ranged from 80 yr at 50 cm to 2000–3000 yr in the bottom layers (430–530 cm). Linear (Cores 5, 5-5, 18, 19, 27, and 31) and exponential (Core 2) models were used in calculations of the downward movement of the DOC, to derive  $d_{doc}$ , as the depth of collection of the POC in Equation (5). The average apparent rate of the DOC downward movement was 0.047 ± 0.019 cm yr<sup>-1</sup>, the range being -0.24–0.97 cm yr<sup>-1</sup>. Negative values mean upward DOC movement, which was found for ten samples (~15%). The minimum (~0.52 cm yr<sup>-1</sup>) and maximum (17.7 cm yr<sup>-1</sup>) values were found in the uppermost 50 cm (Figures 3 and 4). They are likely to be influenced by the experimental errors and calibration uncertainty, giving ±20/30 years for modern dates [59].

## 4. Discussion

The study was aimed at describing the stratigraphy to explore the behaviour of the DOC in a peat profile in Western Siberia and to estimate the apparent rate of the DOC downward movement. The DOC is related to the carbon cycle, redistributing carbon in the peatland and removing its part out [16,60]; it acts as a source for methane and carbon dioxide production [15,17,18,30,31]. Thus, this study contributes to improving our understanding of the carbon cycle by considering the importance of a hitherto neglected long-term carbon flux pathway, along with the implications for the <sup>14</sup>C dating of peatlands, as well as the temporal and spatial variation of greenhouse gas dynamics.

*Sphagnum* peat bogs are dominant in the Middle Taiga zone [5], covering ~28% of the entire zonal area [61] and mostly occupying watersheds. Generally, these peatlands have a similar developmental history, which involves initial waterlogging via paludification or terrestrialisation, resulting in the formation of a eutrophic peat layer, followed by a short stage when the initiation of minerotrophic peat occurred, then an abrupt change to the ombrotrophic stage [1,39,62].

The ACAR, PA, and hydrology of peatlands are all related to the stratigraphy [10]. In this study, it was shown that about two-thirds of the Mukhrino peat body consists of ombrotrophic *Sphagnum* peat with low ash content and low bulk density, which matches existing data for the Western Siberian lowland [6]. These properties are mostly the result of the composition of plant communities from which the peat formed, along with climatic conditions at the time of peat formation, rather than peat age [63]. The similar PA values were found for the Great Vasyugan mire, where the PA was higher for ombrotrophic *Sphagnum* peat (0.115 cm yr<sup>-1</sup>) than for minerotrophic peat (0.059 cm yr<sup>-1</sup>) [64]. These data may be explained by the location in the southern Taiga, which offers the most-favourable meteorological conditions for peatland development [39]. In [58], it was concluded that the

average PA for the Middle Taiga zone was  $0.056 \text{ cm yr}^{-1}$ , whereas the average PA in the southern Taiga zones was  $0.074\text{--}0.08 \text{ cm yr}^{-1}$ . This underlines the importance of different external conditions during peat accumulation.

A linear age–depth model means a continuous peat accumulation process, i.e., the input and decay of organic matter have constant rates; the convex shape shows a peat accumulation decrease at present due to disturbance or unfavourable environmental conditions. The majority of published peat age–depth models showed a concave shape, meaning that decomposition is ongoing in the catotelm [12,65]. This means that most peatlands have a PA rate higher than the decay rate at the moment.

The age–depth models derived for the Mukhrino peatland were almost linear for Cores 19 and 31, and a similar shape was found in Central Europe, but covering only the last 2000 years [66]: s-shaped for Cores 5, 27, and 5-5, similar to Canadian fen [67]; concave (in the case of a reversed x-axis) for Core 2; and broken for Core 18 (Figures 3 and 4). The presence of only one concave model at this peatland may have been caused by the dominance of peat moss (ombrotrophic *Sphagnum*) remains (comprising 90% of the cores), which are the most-resistant bog plant species to decomposition [68]. Despite the different shapes of the age–depth models, all of the carbon accumulation curves had similar positive exponential shapes. It seems that the rate of peat accumulation does not greatly affect the ACAR, which is influenced more strongly by other factors, such as the diversity and biochemical content of vegetation remains, bulk density, carbon content, and local topography and hydrology [56,58,69,70].

Regarding the eutrophic phase of the peatland's development, the peat accumulation process is influenced by the proximity to the mineral soil, which leads to favourable geochemical conditions and fast peat accumulation [71] due to higher litter input [68]. Moreover, fen vegetation is less sensitive to climate conditions and, thus, has more-stable PA values [71]. Nonetheless, the initial rate of mass loss for fen vegetation and increasing age (i.e., longer period of decomposition) result in a lower PA value. When the fen-to-bog succession proceeds to the transitional phase, it features a low PA ( $0.037 \text{ cm yr}^{-1}$ ) and a slow ACAR ( $30.46 \text{ g m}^{-2} \text{ yr}^{-1}$ ). This is probably related to the composition of the vegetation—including the lack of *Sphagnum* species—and high decomposition rates [72]. On the other hand, the highest ACAR values were measured for eutrophic ( $63.1\text{--}48.0 \text{ g m}^{-2} \text{ yr}^{-1}$ ) peat, due to the abundance of grass and woody debris, which is rich in carbon. Ombrotrophic peats consist mostly of the remains of *Sphagnum* mosses, which contain the lowest carbon levels. Thus, the lowest value of the ACAR ( $34.4\text{--}12.1 \text{ g m}^{-2} \text{ yr}^{-1}$ ) was found for ombrotrophic peat.

The contemporary approaches of machine learning can provide powerful tools for the extrapolation and prediction of the peat properties and carbon storage in the peatlands. One of the most-efficient algorithms used in environmental studies is XGBoost [73,74]. With a model ensemble, a model of the focus features is built (for example, the bulk density, ash content, and carbon content in our case). But, this algorithm needs a massive amount of input data. So, existing databases about carbon storage in the peatlands can be used for teaching this algorithm and estimation on a global scale.

In this study, we discovered a clear pattern of age differences between the DOC and POC sampled from the same peat depth. It seems that processes leading to the separation of the DOC and POC occur in the peatland, although the detailed mechanisms are still unclear. Possible reasons for the date differences that can be largely excluded include:

1. Sedge and *Scheuchzeria* roots growing down through the peat to a depth of two metres [34] were not found in any of the dated samples (which were visually controlled); they cannot penetrate into deeper layers. This would cause extreme inversions of the age–depth model (for example, when the modern roots reached ancient peat layers), which were not found in the current study. The roots of trees and dwarf shrubs occupy only the surface aerobic layer because they lack aerenchyma.

2. Cryoturbation causing an intensive and ubiquitous date discrepancy could not occur because permafrost has disappeared from the Middle Taiga zone in recent centuries.

3. Periodic flooding of the Mukhrino peatland should form repeated alluvium layers, of which only one has been detected, in the upper layer.

4. Peat fires, which occur only during extremely hot and dry years in the Taiga zone, do not explain the pattern of DOC and POC ages or the peat profile.

We suppose that the main reason for the age discrepancy is the DOC's downward movement. This would mean there is an additional pathway of carbon efflux from peatland that has not been properly studied so far. Numerous studies have analysed DOC fluxes from peatlands into streamwater [16,25,75,76], but few of these have considered the DOC's downward movement. On the other hand, the process has been considered by the authors who found that the  $^{14}\text{C}$  ages of carbon dioxide and methane are younger than those of the surrounding peat [15,17,18,30,31]. The results from southwest England have shown that the DOC is 830–1260 yr younger than the surrounding peat [18], while ref. [20] published results from a 7 m-deep peatland in Scotland showing age differences between the DOC and the peat that increased with depth from 80 to 1835 yr. One possible explanation is that young DOC, which is transported from the upper to the lower peat layers, is then converted to  $\text{CO}_2$  and  $\text{CH}_4$  by microbial activity.

Only [21] previously took the DOC's downward movement into account for peatlands in Western Siberia, where they recorded a maximum age difference of 6500 years between the DOC and POC. In the study reported here, the difference between the DOC's and POC's ages increased with depth, from 9 to 3044 yr (excluding three negative differences found in the uppermost 50 cm). The date discrepancy appeared at a 100 cm depth, i.e., at the lowest position of the water table (Figures 3 and 4), where no active water flow takes place, and the DOC is, therefore, not affected by mixing with surrounding water layers.

We can suggest several possible causes for the DOC's downward movement and age delay specifically in the Mukhrino peatland:

1. This process might be fostered by the location of the Mukhrino peatland, which occupies the second-highest terrace and is drained by the small rivers "Mukhrina" and "Bolshaya Rechka" located 6–8 m lower from the eastern and western sides. This creates a piezometric gradient (differences in the water heads between the locations), which enables the water from the peatland to penetrate through the mineral bottom (clay layer with hydraulic conductivity in the range of  $10^{-10}$  to  $10^{-6}$   $\text{cm s}^{-1}$  [77]) and discharge to the streams (Figure 2). The water deficit thus created in the lower layers must be compensated by the water influx from the upper peatland horizons, resulting in a vertical flow of water transporting the DOC.

2. The temperature profile measured in the south Taiga zone shows maximum temperature differences of 18 °C between the upper and lower layers of the peat body over the year [78]. This gradient may initiate a convection process, which causes the vertical movement of the mobile phase. The opposite was shown by [79], where the decreased amount of porewater caused by thermal stratification in autumn caused the rapid diffusion of  $\text{CO}_2$  from deeper porewater to the peatland's surface.

3. Reference [80] showed a possible path of methane displacement into deeper soil horizons due to the freezing of thick strata of epigenetic permafrost (a permafrost base lowered into previously deposited sediments). The same mechanism might potentially operate in peatlands since high peat porosity is favourable for vertical water movement. The surface layer of the Mukhrino peatland freezes from the end of September to the beginning of November, and water discharge stops completely at that time. Thus, the peatland becomes a huge reservoir consisting of a high-porosity substrate filled with water and completely confined by the ice pack above. The freezing of water may produce additional pressure, pushing the labile dissolved carbon downwards.

4. Another possible mechanism of the DOC's downward movement is the complete saturation of the pore water by the DOC (i.e., the highest-possible concentration in given conditions), whereby the concentration systematically increases with depth by diffusion. A few publications covered this topic [19,20,81] and reported concentrations of  $\sim 2$   $\text{mmol dm}^{-3}$  at the surface and 6–22  $\text{mmol dm}^{-3}$  at the bottom. However, the information specifically about Western Siberian peatlands is limited, reporting concentrations in the range of 80–860  $\text{mL L}^{-1}$  [55].

5. The negative values of the DOC's movement rate may result from an upward flux, which could be caused by water table movement in the surface layers. The rising water table may catch some of the DOC produced in the lower layers and lift it towards the surface, making the DOC age older than the POC age at the same depth [21]. Several negative DOC movement rates were found in the deeper layers (200–300 cm), which might be caused by methodological flaws in the value calculations when the s-shaped age–depth models for Cores 5 and 27 were approximated by linear regression.

Altogether, these factors may support the hypothesis about the DOC's vertical movement and foster this process. Based on these factors, the DOC's vertical movement process must to be always supported by external forces and stops in its absence. The process seems to be slow, scaling with the diffusion process's velocity, and span over hundreds of years. Studying the factors may help to discover the way of water and DOC redistribution in peatlands, the connection between the peatlands and groundwater, the peatland's processes happening during the winter season when there is no discharge.

In our study, we estimated an average apparent rate of the DOC's downward movement of  $0.047 \pm 0.019$  cm yr<sup>-1</sup>. There was a slight tendency for the rates to decrease, by 2–10-times, towards the mineral bottom. The most likely reason is low vertical hydraulic conductivity in the deep, dense, and well-decomposed basal peat [82]. A limited number of publications estimated the rates of DOC vertical movement, especially for the Russian Federation and Siberia, in particular. Reference [18] used a vertical hydraulic conductivity value of 31.5 cm yr<sup>-1</sup> to estimate the DOC's vertical transport in the U.K. This value exceeded our results by ~600-times because the study was based on potential water movement, which varies significantly with the degree of saturation and due to the physical properties of peat [83]. However, this value might be used as a potential rate of the DOC's downward movement. It has to be regarded as a maximum possible velocity, i.e., as a limiting factor. Anyway, additional study is needed to cover this lack in knowledge in the topic of the DOC's distribution in the peatland.

This result provides a possible explanation for the date delay between the DOC's and POC's ages at the same depth and quantifies the apparent rate of the DOC's vertical movement in Western Siberian ombrotrophic peatlands for the first time. In long-term processes of peatland development during the last 10,000–12,000 yr [7], the DOC's downward movement could potentially make a significant additional contribution to the global carbon cycle and should, therefore, be considered for inclusion in the peatland carbon balance calculation. However, our estimate of the amount of carbon lost through the DOC's vertical movement (28–404 mg m<sup>-2</sup> yr<sup>-1</sup>) is equivalent to only 0.07%–1.07% of the ACAR and 0.4%–5.2% of the average DOC export through runoff [16]. Thus, the vertical movement of the DOC may cause age discrepancies between the mobile (DOC) and immobile (POC) peat fractions at the same depth, but, based on our estimates, it forms an additional flux in the carbon balance of the peatland. Taking into account the area of Western Siberian peatlands, the additional DOC flux may create a significant input to the streams through groundwater flow. This flux should be included in the models predicting the future climate and carbon balance changes.

## 5. Conclusions

In this research, we investigated the typical ombrotrophic peatland located in the Middle Taiga zone of Western Siberia. The peatland age is approximately 10,000 cal. years BP, and it is composed of 2/3 oligotrophic peat in the upper part and eutrophic peat at the bottom. Throughout the entire history of the peatland's development, the average peat accumulation rate was estimated to be  $0.067 \pm 0.018$  cm yr<sup>-1</sup>, and the carbon accumulation rate was  $38.56 \pm 12.21$  g m<sup>-2</sup> yr<sup>-1</sup>. These values might be used to teach machine learning algorithms to increase accuracy and automate the procedure of the carbon accumulation rates and carbon storage estimations.

Using AMS dating of both the DOC and POC, a clear pattern of age differences was found. We hypothesised that the DOC's vertical migration may cause this. However, most

of the factors supporting this idea are theoretical, and additional studies must be carried out. Moreover, the path of the DOC's flux is still unclear, so further investigation, such as stable isotope tracking [84], is necessary.

The Mukhrino field station, functioning as an open-access international science platform year-round, provides an opportunity to conduct a complex study linking together all factors controlling the ecosystem's behaviour. The next research work will be focused on connecting in the model the carbon fluxes [85] with environmental conditions [40] and peatland hydrology [16,60].

**Supplementary Materials:** The following supporting information can be downloaded at: <https://www.mdpi.com/article/10.3390/f14122393/s1>.

**Author Contributions:** Conceptualisation: E.D.L. and E.-D.S.; methodology: E.-D.S., I.K. and E.A.Z.; software: E.A.Z.; investigation: E.A.Z. and I.K.; writing (original draft preparation): E.A.Z. and E.D.L.; writing (review and editing): E.-D.S., I.K., E.D.L. and E.A.Z.; visualisation: E.A.Z.; supervision: E.-D.S. and E.D.L. All authors have read and agreed to the published version of the manuscript.

**Funding:** This research was funded by the state assignment of the Ministry of Science and Higher Education of the Russian Federation to organise a new young researchers Laboratory in Yugra State University (Research number 1022031100003-5-1.5.1) as a part of the implementation of the National Project "Science and universities".

**Data Availability Statement:** Data are contained within the article.

**Acknowledgments:** We sincerely appreciate the support of Konstantin Kudrevatykh, who helped with sampling, passed through the bog, and worked hard, and Olga A. Hopiyainen, who helped with the English language revision.

**Conflicts of Interest:** The authors declare no conflict of interest. The funders had no role in the design of the study; in the collection, analyses, or interpretation of the data; in the writing of the manuscript; nor in the decision to publish the results.

## References

1. Zemtsov, A.A.; Mezentsev, A.V.; Inisheva, L.I. *Bolota Zapadnoj Sibiri: Ikh rol' v Biosfere (Mires of Western Siberia: Their Role in the Bbiosphere)*, 3rd ed.; OOO Tomskiy CNTI: Tomsk, Russia, 2000; p. 72.
2. Xu, J.; Morris, P.J.; Liu, J.; Holden, J. PEATMAP: Refining estimates of global peatland distribution based on a meta-analysis. *Catena* **2018**, *160*, 134–140. [[CrossRef](#)]
3. Yu, Z.; Charman, D.; Beilman, D.W.; Brovkin, V.; Large, D.J. Carbon in peat on Earth through time (C-PEAT). *Past Glob. Chang. Mag.* **2014**, *22*, 99. [[CrossRef](#)]
4. Sheng, Y.; Smith, L.C.; MacDonald, G.M.; Kremenetski, K.V.; Frey, K.E.; Velichko, A.A.; Lee, M.; Beilman, D. Dubinin, P. A high resolution GIS based inventory of the west Siberian peat carbon pool. *Glob. Biogeochem. Cycles* **2004**, *18*, 1–14. [[CrossRef](#)]
5. Peregon, A.; Maksyutov, S.; Kosykh, N.P.; Mironycheva-Tokareva, N.P. Map-based inventory of wetland biomass and net primary production in western Siberia. *J. Geophys. Res. Biogeosci.* **2008**, *113*, G01007. [[CrossRef](#)]
6. Bleuten, W.; Lapshina, E.D. *Carbon Storage and Atmospheric Exchange by West Siberian Peatlands*, 1st ed.; Physical Geography; Utrecht University: Utrecht, The Netherlands; Tomsk State University: Tomsk Oblast, Russia, 2001; p. 116.
7. Kremenetski, K.V.; Velichko, A.A.; Borisova, O.K.; MacDonald, G.M.; Smith, L.C.; Frey, K.E.; Orlova, L.A. Peatlands of the Western Siberian lowlands: Current knowledge on zonation, carbon content and Late Quaternary history. *Quat. Sci. Rev.* **2003**, *22*, 703–723. [[CrossRef](#)]
8. Smith, L.C.; MacDonald, G.M.; Velichko, A.A.; Beilman, D.W.; Borisova, O.K.; Frey, K.E.; Kremenetski, K.V.; Sheng, Y. Siberian peatlands a net carbon sink and global methane source since the early Holocene. *Science* **2004**, *303*, 353–356. [[CrossRef](#)] [[PubMed](#)]
9. Woodwell, G.M.; Mackenzie, F.T.; Houghton, R.A.; Apps, M.; Gorham, E.; Davidson, E. Biotic feedbacks in the warming of the earth. *Clim. Chang.* **1998**, *40*, 518. [[CrossRef](#)]
10. Tsyganov, A.N.; Zarov, E.A.; Mazei, Y.A.; Kulkov, M.G.; Babeshko, K.V.; Yushkovets, S.Y.; Payne, R.J.; Ratcliffe, J.L.; Fatyunina, Y.A.; Zazovskaya, E.P.; et al. Key periods of peatland development and environmental changes in the middle taiga zone of Western Siberia during the Holocene. *Ambio* **2021**, *50*, 1–14. [[CrossRef](#)]
11. Turunen, J.; Tahvanainen, T.; Tolonen, K.; Pitkanen, A. Carbon accumulation in West Siberian mires, Russia. *Glob. Biogeochem. Cycles* **2001**, *15*, 285–296. [[CrossRef](#)]
12. Clymo, R.S.; Turunen, J.; Tolonen, K. Carbon accumulation in peatland. *Oikos* **1998**, *81*, 368–388. [[CrossRef](#)]

13. Feurdean, A.; Gałka, M.; Florescu, G.; Diaconu, A.C.; Tanțău, I.; Kirpotin, S.; Hutchinson, S.M. 2000 years of variability in hydroclimate and carbon accumulation in western Siberia and the relationship with large-scale atmospheric circulation: A multi-proxy peat record. *Quat. Sci. Rev.* **2019**, *226*, 105948. [[CrossRef](#)]
14. Beilman, D.W.; MacDonald, G.M.; Smith, L.C.; Reimer, P.J. Carbon accumulation in peatlands of West Siberia over the last 2000 years. *Glob. Biogeochem. Cycles* **2009**, *23*, GB1012. [[CrossRef](#)]
15. Aravena, R.; Warner, B.G.; Charman, D.J.; Belyea, L.R.; Mathur, S.P.; Dinel, H. Carbon isotopic composition of deep carbon gases in an ombrogenous peatland, northwestern Ontario. *Radiocarbon* **1993**, *35*, 271–276. [[CrossRef](#)]
16. Bleuten, W.; Zarov, E.; Schmitz, O. A high-resolution transient 3-dimensional hydrological model of an extensive undisturbed bog complex in West Siberia. *Mires Peat* **2020**, *26*, 1–25. [[CrossRef](#)]
17. Charman, D.J.; Aravena, R.; Warner, B.G. Carbon dynamics in a forested peatland in north-eastern Ontario, Canada. *J. Ecol.* **1994**, *82*, 55–62. [[CrossRef](#)]
18. Charman, D.J.; Aravena, R.; Bryant, C.L.; Harkness, D.D. Carbon isotopes in peat, DOC, CO<sub>2</sub>, and CH<sub>4</sub> in a Holocene peatland on Dartmoor, Southwest England. *Geology* **1999**, *27*, 539–542. [[CrossRef](#)]
19. Chasar, L.S.; Chanton, J.P.; Glaser, P.H.; Siegel, D.I.; Rivers, J.S. Radiocarbon and stable carbon isotopic evidence for transport and transformation of dissolved organic carbon, dissolved inorganic carbon, and CH<sub>4</sub> in a northern Minnesota peatland. *Glob. Biogeochem. Cycles* **2000**, *14*, 1095–1108. [[CrossRef](#)]
20. Clymo, R.S.; Bryant, C.L. Diffusion and mass flow of dissolved carbon dioxide, methane, and dissolved organic carbon in a 7-m deep raised peat bog. *Geochim. Cosmochim. Acta* **2008**, *72*, 2048–2066. [[CrossRef](#)]
21. Schulze, E.D.; Lapshina, E.; Filippov, I.; Kuhlmann, I.; Mollicone, D. Carbon dynamics in boreal peatlands of the Yenisey region, Western Siberia. *Biogeosciences* **2015**, *12*, 7057–7070. [[CrossRef](#)]
22. Kolka, R.; Weishampel, P.; Fröberg, M. Measurement and importance of dissolved organic carbon. In *Field Measurements for Forest Carbon Monitoring*; Hoover, C.M., Ed.; Springer: Dordrecht, The Netherlands, 2008; pp. 32–58. [[CrossRef](#)]
23. Lim, A.G.; Loiko, S.V.; Kuzmina, D.M.; Krickov, I.V.; Shirokova, L.S.; Kulizhsky, S.P.; Vorobyev, S.N.; Pokrovsky, O.S. Dispersed ground ice of permafrost peatlands: Potential unaccounted carbon, nutrient and metal sources. *Chemosphere* **2021**, *266*, 128953. [[CrossRef](#)]
24. Freeman, C.; Fenner, N.; Ostle, N.J.; Kang, H.; Dowrick, D.J.; Reynolds, B.; Lock, M.A.; Sleep, D.; Hughes, S.; Hudson, J. Export of dissolved organic carbon from peatlands under elevated carbon dioxide levels. *Nature* **2004**, *430*, 195–198. [[CrossRef](#)]
25. Frey, K.E.; Smith, L.C. Amplified carbon release from vast West Siberian peatlands by 2100. *Geophys. Res. Lett.* **2005**, *32*, L09401. [[CrossRef](#)]
26. Schulze, W.X. Protein analysis in dissolved organic matter: What proteins from organic debris, soil leachate and surface water can tell us—A perspective. *Biogeosciences* **2005**, *2*, 75–86. [[CrossRef](#)]
27. Billett, M.F.; Garnett, M.H.; Harvey, F. UK peatland streams release old carbon dioxide to the atmosphere and young dissolved organic carbon to rivers. *Geophys. Res. Lett.* **2007**, *34*, 1–6. [[CrossRef](#)]
28. Raymond, P.A.; Bauer, J.E. Use of <sup>14</sup>C and <sup>13</sup>C natural abundances for evaluating riverine, estuarine, and coastal DOC and POC sources and cycling: A review and synthesis. *Org. Geochem.* **2001**, *32*, 469–485. [[CrossRef](#)]
29. Waddington, J.M.; Roulet, N.T. TGroundwater flow and dissolved carbon movement in a boreal peatland. *J. Hydrol.* **1997**, *191*, 122–138. [[CrossRef](#)]
30. Aravena, R.; Wassenaar, L.I. Dissolved organic carbon and methane in a regional confined aquifer, southern Ontario, Canada: Carbon isotope evidence for associated subsurface sources. *Appl. Geochem.* **1993**, *8*, 483–493. [[CrossRef](#)]
31. Chanton, J.P.; Bauer, J.E.; Glaser, P.A.; Siegel, D.I.; Kelley, C.A.; Tyler, S.C.; Romanowicz, E.H.; Lazrus, A. Radiocarbon evidence for the substrates supporting methane formation within northern Minnesota peatlands. *Geochim. Cosmochim. Acta* **1995**, *59*, 3663–3668. [[CrossRef](#)]
32. Kołaczek, P.; Gałka, M.; Lamentowicz, M.; Marcisz, K.; Kajukalo-Drygalska, K.; Karpińska-Kołaczek, M. Increased radiocarbon dating resolution of ombrotrophic peat profiles reveals periods of disturbance which were previously undetected. *Quat. Geochronol.* **2019**, *52*, 21–28. [[CrossRef](#)]
33. Lamentowicz, M.; Słowiński, M.; Marcisz, K.; Zielińska, M.; Kaliszan, K.; Lapshina, E.; Gilbert, D.; Buttler, A.; Fiałkiewicz-Kozieł, B.; Jassey, V.E.J.; et al. Hydrological dynamics and fire history of the last 1300 years in western Siberia reconstructed from a high-resolution, ombrotrophic peat archive. *Quat. Res.* **2015**, *84*, 312–325. [[CrossRef](#)]
34. Glaser, P.H.; Volin, J.H.; Givnish, T.J.; Hansen, B.C.S.; Stricker, C.A. Carbon and sediment accumulation in the Everglades (USA) during the past 4000 years: Rates, drivers, and sources of error. *J. Geophys. Res. Biogeosci.* **2012**, *117*, G03026. [[CrossRef](#)]
35. Jaworski, T.; Niewiarowski, W. Frost peat mounds on Hermansenøya (Oscar II Land, NW Svalbard)—Their genesis, age and terminology. *Boreas* **2012**, *41*, 660–672. [[CrossRef](#)]
36. Turetsky, M.R.; Donahue, W.; Benscoter, B.W. Experimental drying intensifies burning and carbon losses in a northern peatland. *Nat. Commun.* **2011**, *2*, 1–5. [[CrossRef](#)]
37. Väiliranta, M.; Oinonen, M.; Seppä, H.; Korkkonen, S.; Juutinen, S.; Tuittila, E.S. Unexpected problems in AMS <sup>14</sup>C dating of fen peat. *Radiocarbon* **2014**, *56*, 95–108. [[CrossRef](#)]
38. Gvozdetkii, N.A.; Krivolutskii, A.E.; Makunina, A.A. *Fiziko-Geograficheskoe Rajonirovanie Tyumenskoy Oblasti (Physical and Geographical Zoning of the Tyumen Region)*; Moscow State University Publishing House: Moscow, Russia, 1973; pp. 9–28. (In Russian)

39. Ivanov, K.E.; Novikov, S.M. *Bolota Zapadnoj Sibiri ih Stroenie i Gidrologicheskij Rezhim (Peatlands of Western Siberia, Their Structure and Hydrological Regime)*; Gidrometeoizdat: Leningrad, Russia, 1976; 447p.
40. Dyukarev, E.; Filippova, N.; Karpov, D.; Shnyrev, N.; Zarov, E.; Filippov, I.; Voropay, N.; Avilov, V.; Artamonov, A.; Lapshina, E. Hydrometeorological dataset of West Siberian boreal peatland: A 10-year record from the Mukhrino Field Station. *Earth Syst. Sci. Data* **2021**, *13*, 2595–2605. [[CrossRef](#)]
41. Filippov, I.V.; Lapshina, E.D. Peatland unit types of lake-bog systems in the Middle Priob'ie (Western Siberia). *Dyn. Environ. Glob. Clim. Chang.* **2008**, *1*, 115–124. [[CrossRef](#)]
42. Mauquoy, D.; Hughes, P.D.M.; Van Geel, B. A protocol for plant macrofossil analysis of peat deposits. *Mires Peat* **2010**, *7*, 1–5. Available online: <https://hdl.handle.net/11245/1.345803> (accessed on 26 November 2023).
43. Mauquoy, D.; Van Geel, B. Plant macrofossil methods and studies: Mire and peat macros. *Encycl. Quat. Sci.* **2013**, *113*, 637–656. [[CrossRef](#)]
44. Matukhin, R.G.; Matukhina, V.G.; Vasiliev, I.P.; Mikhantjeva, L.S.; Popova, G.I.; Markov, D.V.; Ospennikova, L.A.; Skobeeva, E.I. *Klassifikatsiya Torfov i Torfyanykh Zalezhey Zapadnoj Sibiri (Classification of Peat Types and Peat Deposits of West Siberia)*, 1st ed.; NITS OIGGM: Novosibirsk, Russia, 2000; p. 90.
45. Steinhof, A. Accelerator Mass Spectrometry of Radiocarbon. In *Radiocarbon and Climate Change*; Schuur, E.A., Druffel, E.R., Trumbore, S.E., Eds.; Springer International Publishing: Cham, Switzerland, 2016; pp. 253–278.
46. Steinhof, A.; Altenburg, M.; Machts, H. Sample preparation at the Jena <sup>14</sup>C laboratory. *Radiocarbon* **2017**, *59*, 815–830. [[CrossRef](#)]
47. Reimer, P.J.; Austin, W.E.N.; Bard, E.; Bayliss, A.; Blackwell, P.G.; Ramsey, C.B.; Butzin, M.; Cheng, H.; Edwards, R.L.; Friedrich, M.; et al. The IntCal20 Northern Hemisphere Radiocarbon Age Calibration Curve (0–55 cal kBP). *Radiocarbon* **2020**, *62*, 725–757. [[CrossRef](#)]
48. Hua, Q.; Barbetti, M.; Rakowski, Z. Atmospheric radiocarbon for the period 1950–2010. *Radiocarbon* **2013**, *55*, 2059–2072. [[CrossRef](#)]
49. Blaauw, M. Clam: Classical Age-Depth Modelling of Cores from Deposits. R Package. Available online: <https://cran.r-project.org/web/packages/clam/index.html> (accessed on 22 September 2023).
50. Blaauw, M.; Christen, J.A.; Aquino, M.A. Rbacon: Age-Depth Modelling Using Bayesian Statistics. R Package Version 2.4.2. Available online: <https://cran.r-project.org/web/packages/rbacon/index.html> (accessed on 22 September 2023).
51. Turunen, J.; Tomppo, E.; Tolonen, K.; Reinikainen, A. Estimating carbon accumulation rates of undrained mires in Finland—application to boreal and subarctic regions. *Holocene* **2002**, *12*, 69–80. [[CrossRef](#)]
52. Łopatka, A.; Siebielec, G.; Kaczyński, R.; Stuczynski, T. Analysis of Soil Carbon Stock Dynamics by Machine Learning—Polish Case Study. *Land* **2023**, *12*, 1587. [[CrossRef](#)]
53. Borren, W.; Bleuten, W.; Lapshina, E.D. Holocene peat and carbon accumulation rates in the southern taiga of western Siberia. *Quat. Res.* **2004**, *61*, 42–51. [[CrossRef](#)]
54. Fraser, C.J.D.; Roulet, N.T.; Moore, T.R. Hydrology and dissolved organic carbon biogeochemistry in an ombrotrophic bog. *Hydrol. Process.* **2001**, *15*, 3151–3166. [[CrossRef](#)]
55. Shaniova, V.S. Approaches to determining the content of dissolved organic carbon in peat (Podkhody k opredeleniu sodержaniya rastvorenogo organicheskogo ugleroda v torfe). *Bizn.-Transform. Upr. Ulučsheniyami* **2023**, *1*, 31–37.
56. Lapshina, E.D.; Pologova, N.N.; Muldiyarov, E.Y. Pattern of development and carbon accumulation in homogenous Sphagnum fuscum peat deposit on the south of West Siberia. In Proceedings of the International Field Symposium West Siberian Peatlands and Carbon Cycle: Past and Present, Noyabrsk, Russia, 18–22 August 2001; pp. 101–104.
57. Loisel, J.; Yu, Z.; Beilman, D.W.; Camill, P.; Alm, J.; Amesbury, M.J.; Matthew, J.; Anderson, S.; Bochicchio, C.; Barber, K.; et al. A database and synthesis of northern peatland soil properties and Holocene carbon and nitrogen accumulation. *Holocene* **2014**, *24*, 1028–1042. [[CrossRef](#)]
58. Lapshina, E.D. Peat grow dynamic on the bogs of taiga zone of West Siberia. In Proceedings of the West Siberian Peatlands and Carbon Cycle: Past and Present Conference, Novosibirsk, Russia, 7–27 June 2011; pp. 38–39.
59. Hajdas, I.; Ascough, P.; Garnett, M.H.; Fallon, S.J.; Pearson, C.L.; Quarta, G.; et al. Radiocarbon dating. *Nat. Rev. Methods Prim.* **2021**, *1*, 62. . [[CrossRef](#)]
60. Zarov, E.A.; Meshcheryakova, A.V.; Shanyova, V.S.; Khoroshavin, V.Y. Water table and dissolved organic carbon seasonal dynamic at the different ecosystems of the ombrotrophic bog (Mukhrino, West Siberia). *Smart Sustain. Cities Conf.* **2022**, 169–180.
61. Terentjeva, I.E.; Glagolev, M.V.; Lapshina, E.D.; Sabrekov, A.F.; Maksyutov, S. Mapping of West Siberian taiga wetland complexes using Landsat imagery: Implications for methane emissions. *Biogeosciences* **2016**, *13*, 4615–4626. [[CrossRef](#)]
62. Liss, O.L.; Abramova, L.I.; Avetov, N.A.; Berezina, N.A.; Inisheva, L.I.; Kurnishkova, T.V.; Sluka, Z.A.; Tolpysheva, T.Y.; Shvedchikova N.K. *Bolotnye Sistemy Zapadnoj Sibiri i ih Prirodoohrannoe Znachenie (Mire Systems of Western Siberia and Their Nature Conservation Value)*, 1st ed.; Grif i Ko: Tula, Russia, 2001; 584p.
63. Chambers, F.; Beilman, D.; Yu, Z. Methods for determining peat humification and for quantifying peat bulk density, organic matter and carbon content for palaeostudies of climate and peatland carbon dynamics. *Mires Peat* **2010**, *7*, 1–10.
64. Pologova, N.N.; Lapshina, E.D. Nakoplenie ugleroda v torfyanykh zalezhah Bol'shogo Vasyuganskogo bolota (Carbon accumulation in peat deposits of the Great Vasyugan mire). In *IV Sobranie po Klimatoekologicheskomu Monitoringu (The Fourth Climate-Ecological Monitoring Meeting)*; Dyukarev, A.G., Ed.; Publishing House: Tomsk, Russia, 2001; pp. 72–73.
65. Yu, Z.; Campbell, I.D.; Vitt, D.H.; Apps, M.J. Modelling long-term peatland dynamics. I. Concepts, review, and proposed design. *Ecol. Model.* **2001**, *145*, 197–210. [[CrossRef](#)]

66. Fiałkiewicz-Kozieł, B.; Kołaczek, P.; Piotrowska, N.; Michczyński, A.; Łokas, E.; Wachniew, P.; Woszczyk, M.; Sensuła, B. High-resolution age-depth model of a peat bog in Poland as an important basis for paleoenvironmental studies. *Radiocarbon* **2014**, *56*, 109–125. [[CrossRef](#)] [[PubMed](#)]
67. O'Reilly, B.C. Paleocological and Carbon Accumulation Dynamics of a Fen Peatland in the Hudson Bay Lowlands, Northern Ontario, from the Mid-Holocene to Present. Ph.D. Thesis, University of Toronto, Toronto, ON, Canada, 2011; Volume 113, 132p.
68. Thormann, M.N.; Szumigalski, A.R.; Bayley, S.E. Aboveground peat and carbon accumulation potentials along a bog-fen-marsh wetland gradient in southern boreal Alberta, Canada. *Wetlands* **1999**, *19*, 305–317. [[CrossRef](#)]
69. Lapshina, E.D.; Pologova, N.N. Spatial dynamics of peat grows and carbon accumulation in *Sphagnum* bogs (boreal West Siberia). In Proceedings of the West Siberian Peatlands and Carbon Cycle: Past and Present Conference, Novosibirsk, Russia, 7–27 June 2011; Vomperskiy, S.E., Ed.; pp. 96–98.
70. Pologova, N.N.; Lapshina, E.D. Nakoplenie ugleroda v torfyanyh zalezah Bol'shogo Vasyuganskogo bolota (Carbon accumulation in peat deposits of the Great Vasyugan mire). In *Bolshoe Vasyuganskoe Boloto. Sovremennoe Sostoyanie i Processy Razvitiya (Great Vasyugan Mire. Actual Statement and Development Processes)*; Kabanov, M.V., Ed.; ISA SO RAN: Tomsk, Russia, 2002; pp. 174–179.
71. Frolking, S.; Roulet, N.T.; Moore, T.R.; Richard, P.J.; Lavoie, M.; Müller, S.D. Modeling northern peatland decomposition and peat accumulation. *Ecosystems* **2001**, *4*, 479–498. [[CrossRef](#)]
72. van Bellen, S.; Garneau, M.; Booth, R.K. Holocene carbon accumulation rates from three ombrotrophic peatlands in boreal Quebec, Canada: Impact of climate-driven ecohydrological change. *Holocene* **2011**, *21*, 1217–1231. . [[CrossRef](#)]
73. Hikouei, I.S.; Eshleman, K.N.; Saharjo, B.H.; Graham, L.L.; Applegate, G.; Cochrane, M.A. Using machine learning algorithms to predict groundwater levels in Indonesian tropical peatlands. *Sci. Total Environ.* **2023**, *857*, 159701. [[CrossRef](#)]
74. Bartold, M.; Kluczek, M. A Machine Learning Approach for Mapping Chlorophyll Fluorescence at Inland Wetlands. *Remote Sens.* **2023**, *15*, 2392. [[CrossRef](#)]
75. Buzek, F.; Novak, M.; Cejkova, B.; Jackova, I.; Curik, J.; Veselovsky, F.; Stpanova, M.; Bohdalkova, L. Assessing DOC export from a Sphagnum dominated peatland using  $\sigma_{13}C$  and  $\sigma_{18}O-H_2O$  stable isotopes. *Hydrol. Process.* **2019**, *33*, 2792–2803. [[CrossRef](#)]
76. Freeman, C.; Evans, C.D.; Monteith, D.T.; Reynolds, B.; Fenner, N. Export of organic carbon from peat soils. *Nature* **2001**, *412*, 785. [[CrossRef](#)]
77. Coduto, D.P. *Geotechnical Engineering: Principles and Practices*, 2nd ed.; Prentice-Hall: Englewood Cliffs, NJ, USA, 1999; p. 800.
78. Kiselev, M.V.; Dyukarev, E.A.; Voropay, N.N. Features of seasonal temperature variations in peat soils of oligotrophic bogs in south taiga of Western Siberia. *IOP Conf. Ser. Earth Environ. Sci.* **2018**, *138*, 012006. [[CrossRef](#)]
79. Campeau, A.; Vachon, D.; Bishop, K.; Nilsson, M.B.; Wallin, M.B. Autumn destabilization of deep porewater CO<sub>2</sub> store in a northern peatland driven by turbulent diffusion. *Nat. Commun.* **2021**, *12*, 6857. [[CrossRef](#)]
80. Kraev, G.; Schulze, E.D.; Yurova, A.; Kholodov, A.; Chuvilin, E.; Rivkina, E. Cryogenic displacement and accumulation of biogenic methane in frozen soils. *Atmosphere* **2017**, *8*, 105. [[CrossRef](#)]
81. Cole, L.; Bardgett, R.D.; Ineson, P.; Adamson, J.K. Relationships between enchytraeid worms (Oligochaeta), climate change, and the release of dissolved organic carbon from blanket peat in northern England. *Soil Biol. Biochem.* **2002**, *34*, 599–607. [[CrossRef](#)]
82. Beckwith, C.W.; Baird, A.J.; Heathwaite, A.L. Anisotropy and depth related heterogeneity of hydraulic conductivity in a bog peat. I: Laboratory measurements. *Hydrol. Process.* **2003**, *17*, 89–101. [[CrossRef](#)]
83. Chason, D.B.; Siegel, D.I. Hydraulic conductivity and related physical properties of peat, Lost River Peatland, northern Minnesota. *Soil Sci.* **1986**, *142*, 91–99. [[CrossRef](#)]
84. Levy, Z.F.; Siegel, D.I.; Dasgupta, S.S.; Glaser, P.H.; Welker, J.M. Stable isotopes of water show deep seasonal recharge in northern bogs and fens. *Hydrol. Process.* **2014**, *28*, 4938–4952. [[CrossRef](#)]
85. Dyukarev, E.A.; Godovnikov, E.A.; Karpov, D.V.; Kurakov, S.A.; Lapshina, E.D.; Filippov, I.V.; Filippova, N.V.; Zarov, E.A. Net ecosystem exchange, gross primary production and ecosystem respiration in ridge-hollow complex at Mukhrino bog. *Geogr. Environ. Sustain.* **2021**, *12*, 227–244. [[CrossRef](#)]

**Disclaimer/Publisher's Note:** The statements, opinions and data contained in all publications are solely those of the individual author(s) and contributor(s) and not of MDPI and/or the editor(s). MDPI and/or the editor(s) disclaim responsibility for any injury to people or property resulting from any ideas, methods, instructions or products referred to in the content.